Search for $D^0 \to K_S^0 K^- e^+ \nu_e$, $D^+ \to K_S^0 K_S^0 e^+ \nu_e$, and $D^+ \to K^+ K^- e^+ \nu_e$

M. Ablikim *et al.*[*]
(BESIII Collaboration)

(Received 14 December 2023; accepted 28 February 2024; published 5 April 2024)

A search has been performed for the semileptonic decays $D^0 \to K_S^0 K^- e^+ \nu_e$, $D^+ \to K_S^0 K_S^0 e^+ \nu_e$, and $D^+ \to K^+ K^- e^+ \nu_e$, using 7.9 fb^{-1} of e^+e^- annihilation data collected at the center-of-mass energy $\sqrt{s} = 3.773$ GeV by the BESIII detector operating at the BEPCII collider. No significant signals are observed, and upper limits are set at the 90% confidence level of 2.13×10^{-5}, 1.54×10^{-5}, and 2.10×10^{-5} for the branching fractions of $D^0 \to K_S^0 K^- e^+ \nu_e$, $D^+ \to K_S^0 K_S^0 e^+ \nu_e$, and $D^+ \to K^+ K^- e^+ \nu_e$, respectively.

DOI: 10.1103/PhysRevD.109.072003

I. INTRODUCTION

The semileptonic decays of charmed mesons offer a clean environment to explore the strong and weak interactions in the charm sector. Over the years, the semileptonic decays of D mesons into pseudoscalar and vector mesons have been investigated extensively by various experiments, such as MARKIII, BESII, CLEO-c, *BABAR*, Belle, LHCb, and BESIII, and their findings are comprehensively summarized in Ref. [1]. In contrast, experimental studies of semileptonic decays involving scalar mesons are relatively limited. The investigations of semileptonic D meson decays involving the light scalar meson $a_0(980)$, which was proposed to be a hadronic molecule composed of $\pi\eta$ or $K\bar{K}$ [2–5], can help to test the theoretical calculations and provide an opportunity to explore the nature and decay properties of $a_0(980)$. Tests on different theoretical calculations are important to explore the realization of chiral symmetry in the low-energy region, and are therefore highly desirable for nonperturbative QCD research [6].

In 2018, the BESIII collaboration reported the observation of the semileptonic decays $D \to a_0(980) e^+ \nu_e$ with $a_0(980) \to \pi\eta$ [7], with branching fractions (BFs) comparable to theoretical expectations [8]. Knowing the product BFs of $D \to a_0(980) e^+ \nu_e$ with $a_0(980) \to \pi\eta$, it is possible to predict the product BFs of $D \to a_0(980) e^+ \nu_e$ with $a_0(980) \to K\bar{K}$ according to $\mathcal{B}(a_0(980) \to K\bar{K}) / \mathcal{B}(a_0(980) \to \eta\pi) = 0.172 \pm 0.019$ [1], and outlined in Table I. Figure 1 shows the tree-level Feynman diagrams of $D^0 \to K_S^0 K^- e^+ \nu_e$, $D^+ \to K_S^0 K_S^0 e^+ \nu_e$, and $D^+ \to K^+ K^- e^+ \nu_e$. These decay processes can be reconstructed using charged tracks alone, providing a cleaner environment for studying the $a_0(980)$ meson [7,9].

In this paper, we present the first searches for the semileptonic decays $D^0 \to K_S^0 K^- e^+ \nu_e$, $D^+ \to K_S^0 K_S^0 e^+ \nu_e$, and $D^+ \to K^+ K^- e^+ \nu_e$. This analysis is based on data samples collected by the BESIII detector at a center-of-mass energy of $\sqrt{s} = 3.773$ GeV in 2010, 2011, and 2021, corresponding to a total integrated luminosity of 7.9 fb^{-1} [10]. Throughout this paper, charge-conjugate channels are always implied.

II. BESIII DETECTOR AND MONTE CARLO SIMULATION

The BESIII detector [11] records symmetric e^+e^- collisions provided by the BEPCII storage ring [12] in the center-of-mass energy range from 2.00 to 4.95 GeV, with a peak luminosity of 1×10^{33} cm^{-2} s^{-1} achieved at $\sqrt{s} = 3.77$ GeV. BESIII has collected large data samples in this energy region [13–15]. The cylindrical core of the BESIII detector [16] covers 93% of the full solid angle and consists of a helium-based multilayer drift chamber (MDC), a plastic scintillator time-of-flight system (TOF), and a CsI(Tl) electromagnetic calorimeter (EMC), which are all enclosed in a superconducting solenoidal magnet providing a 1.0 T magnetic field.

The solenoid is supported by an octagonal flux-return yoke with resistive plate counter muon identification modules interleaved with steel. The charged-particle momentum resolution at 1 GeV/c is 0.5%, and the dE/dx resolution is 6% for electrons from Bhabha scattering. The EMC measures photon energies with a resolution of 2.5% (5%) at 1 GeV in the barrel (end cap) region. The time resolution in the TOF barrel region is 68 ps, while that in the end cap region was 110 ps. The end cap TOF system was upgraded in 2015 using multigap resistive plate chamber technology, providing a time resolution of 60 ps, which benefits 83% of the data used in this analysis [17].

[*]Full author list given at the end of the article.

Published by the American Physical Society under the terms of the Creative Commons Attribution 4.0 International license. Further distribution of this work must maintain attribution to the author(s) and the published article's title, journal citation, and DOI. Funded by SCOAP³.

TABLE I. The measured product BFs of $D \to a_0(980)e^+\nu_e$ with $a_0(980) \to \eta\pi$ and the expected BFs of $D \to a_0(980)e^+\nu_e$ with $a_0(980) \to K\bar{K}$.

BFs	$a_0(980)[\to \pi\eta]e^+\nu_e$ [7] $(\times 10^{-4})$	$a_0(980)[\to K_S^0K^-]e^+\nu_e$ $(\times 10^{-5})$	$a_0(980)[\to K_S^0K_S^0]e^+\nu_e$ $(\times 10^{-5})$	$a_0(980)[\to K^+K^-]e^+\nu_e$ $(\times 10^{-5})$
D^0	$1.33^{+0.33}_{-0.29} \pm 0.09$	$1.14^{+0.28}_{-0.24} \pm 0.07$	$\cdots$	$\cdots$
D^+	$1.66^{+0.81}_{-0.66} \pm 0.11$	$\cdots$	$0.71^{+0.34}_{-0.28} \pm 0.05$	$2.86^{+1.39}_{-1.13} \pm 0.19$

Simulated event samples produced with the Geant4-based [18] Monte Carlo (MC) package which includes the geometric description of the BESIII detector and the detector response, are used to determine the detection efficiency and estimate the backgrounds. The simulation includes the beam-energy spread and initial-state radiation in the e^+e^- annihilations modeled with the generator KKMC [19]. The inclusive MC sample includes the production of $D\bar{D}$ pairs (including quantum coherence for the neutral D channels), the non-$D\bar{D}$ decays of the $\psi(3770)$, the initial-state radiation production of the J/ψ and $\psi(3686)$ states, and the continuum processes incorporated in KKMC [19]. All particle decays are modelled with EvtGen [20] using the BFs either taken from the Particle Data Group [1], when available, or otherwise estimated with LUNDCHARM [21]. Final-state radiation from charged particles is incorporated with the PHOTOS package [22]. In this paper, the inclusive MC sample is used to determine the selection efficiencies and estimate the backgrounds.

The semileptonic decays $D^0 \to K_S^0K^-e^+\nu_e$, $D^+ \to K_S^0K_S^0e^+\nu_e$, and $D^+ \to K^+K^-e^+\nu_e$ are simulated with a generator developed by BESIII specifically for this analysis, where the Flatté formula is used to describe the $a_0(980)$ resonance. This specialized generator is adopted to model the contribution of an intermediate $a_0(980)$, as a general generator may not be suitable. The Flatté formula takes into account the mass, width, and coupling constants of the resonance to calculate its contribution to the decay rates. The mass of the $a_0(980)$ resonance is fixed at 0.990 GeV$/c^2$, while the two coupling constants coupled to $\eta\pi$ (g1) and $K\bar{K}$ (g2) are fixed at 0.341 $(\mathrm{GeV}/c^2)^2$ and 0.304 $(\mathrm{GeV}/c^2)^2$, respectively, as determined in Refs. [23–25].

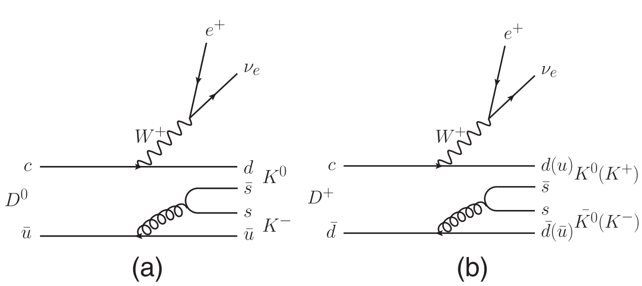

FIG. 1. Tree-level Feynman diagrams of (a) $D^0 \to a_0(980)^-e^+\nu_e$ and (b) $D^+ \to a_0(980)e^+\nu_e$.

III. METHOD

At $\sqrt{s} = 3.773$ GeV, the $D^0\bar{D}^0$ or D^+D^- meson pairs are produced from $\psi(3770)$ decays without accompanying hadrons, which provides an ideal opportunity to study semileptonic decays of D mesons using the double-tag (DT) method [26]. In the first step of the analysis, the single-tag (ST) $\bar{D}^0$ mesons are reconstructed via the hadronic-decay modes of $\bar{D}^0 \to K^+\pi^-$, $K^+\pi^-\pi^0$, and $K^+\pi^-\pi^-\pi^+$; while the ST D^- mesons are reconstructed via the decays $D^- \to K^+\pi^-\pi^-$, $K_S^0\pi^-$, $K^+\pi^-\pi^-\pi^0$, $K_S^0\pi^-\pi^0$, $K_S^0\pi^+\pi^-\pi^-$, and $K^+K^-\pi^-$. Then the semileptonic decays of D meson candidates are reconstructed with the remaining tracks which have not been used in the ST selection. The event, in which the semileptonic decays $D^0 \to K_S^0K^-e^+\nu_e$, $D^+ \to K_S^0K_S^0e^+\nu_e$, or $D^+ \to K^+K^-e^+\nu_e$ are reconstructed in the systems recoiling against the ST $\bar{D}$ mesons, is called a DT event. The product BFs of $D^0 \to K_S^0K^-e^+\nu_e$, $D^+ \to K_S^0K_S^0e^+\nu_e$, and $D^+ \to K^+K^-e^+\nu_e$ are determined by

$$\mathcal{B}_{\mathrm{SL}} = \frac{N_{\mathrm{DT}}}{N_{\mathrm{ST}}^{\mathrm{tot}}\bar{\epsilon}_{\mathrm{sig}}(\mathcal{B}_{K_S^0})^k}, \tag{1}$$

where $N_{\mathrm{ST}}^{\mathrm{tot}}$ and N_{DT} are the yields of the ST $\bar{D}^0(D^-)$ mesons and the DT signal events in data, respectively; $\mathcal{B}_{K_S^0}$ is the BF of $K_S^0 \to \pi^+\pi^-$ quoted from the Particle Data Group [1]; k is the number of K_S^0 mesons in the final state of DT side, and $\bar{\epsilon}_{\mathrm{sig}}$ is the average signal efficiency weighted by the measured yields of tag modes i in the data, i.e.,

$$\bar{\epsilon}_{\mathrm{sig}} = \frac{\sum_i (N_{\mathrm{ST}}^i \cdot \epsilon_{\mathrm{DT}}^i/\epsilon_{\mathrm{ST}}^i)}{N_{\mathrm{ST}}^{\mathrm{tot}}}, \tag{2}$$

where N_{ST}^i are the yields of the ST candidates observed in data, ϵ_{ST}^i is the efficiency of reconstructing the ST mode i (referred to as the ST efficiency), and ϵ_{DT}^i is the efficiency of finding the ST mode i and the $D^0 \to K_S^0K^-e^+\nu_e$, $D^+ \to K_S^0K_S^0e^+\nu_e$, and $D^+ \to K^+K^-e^+\nu_e$ decay simultaneously (referred to as the DT efficiency).

IV. SINGLE TAG SELECTION

Charged tracks detected in the MDC (except for those used for K_S^0 reconstruction) are required to be within a polar angle (θ) range of $|\cos\theta| < 0.93$, where θ is defined with respect to the z axis, which is the symmetry axis of the MDC. The distance of closest approach to the interaction point (IP) along the z axis, $|V_z|$, must be less than 10 cm, and in the transverse plane, $|V_{xy}|$, less than 1 cm. Particle identification (PID) for charged tracks combines measurements of the specific ionization energy loss in the MDC ($\mathrm{d}E/\mathrm{d}x$) and the flight time in the TOF to form likelihoods $\mathcal{L}(h)(h = p, K, \pi)$ for each hadron h hypothesis. Charged kaons and pions are identified by comparing the likelihoods for the kaon and pion hypotheses, $\mathcal{L}(K) > \mathcal{L}(\pi)$ and $\mathcal{L}(\pi) > \mathcal{L}(K)$, respectively.

Each K_S^0 candidate is reconstructed from two oppositely charged tracks satisfying $|V_z| < 20$ cm. The two charged tracks are assigned as $\pi^+\pi^-$ without imposing PID criteria. They are constrained to originate from a common vertex, requiring an invariant mass within $(0.487, 0.511)$ GeV$/c^2$. The decay length of the K_S^0 candidate is required to be separated from the IP by more than twice the vertex resolution, which encompasses both the primary and secondary vertices. The quality of the vertex fits (primary-vertex fit and secondary-vertex fit) is ensured by a requirement on the χ^2 ($\chi^2 < 100$).

Photon candidates are identified using showers in the EMC. The π^0 candidates with both photons from the end cap are rejected because of poor resolution. The deposited energy of each shower must be more than 25 MeV in the barrel region ($|\cos\theta| < 0.80$) and more than 50 MeV in the end cap region ($0.86 < |\cos\theta| < 0.92$). Showers are required to be separated from other charged tracks by an angle greater than 10° in order to eliminate activity induced by tracks. To suppress electronic noise and showers unrelated to the event, the difference between the EMC time and the event start time is required to be within [0, 700] ns. For π^0 candidates, the invariant mass of the photon pair is required to be within $(0.115, 0.150)$ GeV$/c^2$. To improve the resolution, a kinematic fit is performed, where the diphoton invariant mass is constrained to the known π^0 mass [1], and the χ^2 of the fit is required to be less than 50. The momenta obtained from the kinematic fit are used in the subsequent analysis.

In the selection of $\bar{D}^0 \to K^+\pi^-$ candidates, the backgrounds from cosmic rays and Bhabha events are rejected by using the same requirements described in Ref. [27]. The two charged tracks must have a TOF time difference of less than 5 ns. They must not be consistent with being a muon or electron-positron pair. Additionally, there must be at least one EMC shower with energy deposited larger than 50 MeV, or at least one additional charged track detected in the MDC.

To separate the ST $\bar{D}$ mesons from combinatorial backgrounds, we define the energy difference $\Delta E \equiv E_{\bar{D}} - E_{\mathrm{beam}}$ and the beam-constrained mass $M_{\mathrm{BC}} \equiv \sqrt{E_{\mathrm{beam}}^2/c^4 - |\vec{p}_{\bar{D}}|^2/c^2}$, where E_{beam} is the beam energy, and $E_{\bar{D}}$ and $\vec{p}_{\bar{D}}$ are the total energy and momentum of the $\bar{D}$ candidate in the e^+e^- center-of-mass frame, respectively. If there is more than one $\bar{D}$ candidate in a given ST mode, then that candidate with the smallest value of $|\Delta E|$ is kept for the subsequent analysis. The ΔE requirements and ST efficiencies are listed in Table II.

TABLE II. The ΔE requirements, the measured ST $\bar{D}$ yields in the data (N_{ST}^i), and the ST efficiencies (ϵ_{ST}^i) for nine tag modes. The uncertainties are statistical only.

Tag mode	ΔE (GeV)	N_{ST}^i ($\times 10^3$)	ϵ_{ST}^i (%)
$\bar{D}^0 \to K^+\pi^-$	$(-0.027, 0.027)$	1449.5 ± 1.2	64.95 ± 0.01
$\bar{D}^0 \to K^+\pi^-\pi^0$	$(-0.062, 0.049)$	2913.1 ± 2.0	35.52 ± 0.00
$\bar{D}^0 \to K^+\pi^-\pi^-\pi^+$	$(-0.026, 0.024)$	1944.1 ± 1.5	40.42 ± 0.01
$D^- \to K^+\pi^-\pi^-$	$(-0.025, 0.024)$	2164.0 ± 1.5	51.17 ± 0.01
$D^- \to K_S^0\pi^-$	$(-0.025, 0.026)$	250.4 ± 0.5	50.63 ± 0.02
$D^- \to K^+\pi^-\pi^-\pi^0$	$(-0.057, 0.046)$	689.0 ± 1.1	25.50 ± 0.01
$D^- \to K_S^0\pi^-\pi^0$	$(-0.062, 0.049)$	558.4 ± 0.9	26.28 ± 0.01
$D^- \to K_S^0\pi^-\pi^-\pi^+$	$(-0.028, 0.027)$	300.5 ± 0.6	28.97 ± 0.01
$D^- \to K^+K^-\pi^-$	$(-0.024, 0.023)$	187.3 ± 0.5	41.06 ± 0.02

The ST yields are extracted by performing unbinned maximum likelihood fits to the corresponding M_{BC} distribution. In the fit, the signal shape is derived from the MC-simulated signal shape convolved with a double-Gaussian function to compensate for the resolution difference between the data and MC simulation. The background shape is described by the ARGUS function [28], with the end point parameter fixed at 1.8865 GeV$/c^2$ corresponding to E_{beam}. Figure 2 shows the fits to the M_{BC} distributions of the accepted ST candidates in data for different ST modes. The candidates with M_{BC} within $(1.859, 1.873)$ GeV$/c^2$ for $\bar{D}^0$ tags and $(1.863, 1.877)$ GeV$/c^2$ for D^- tags are kept for further analyses. Summing over the tag modes gives the total yields of ST $\bar{D}^0$ and D^- mesons to be $(6306.8 \pm 2.8_{\mathrm{stat}}) \times 10^3$ and $(4149.9 \pm 2.3_{\mathrm{stat}}) \times 10^3$, respectively.

V. DOUBLE TAG SELECTION

The candidates for $D^0 \to K_S^0 K^- e^+ \nu_e$, $D^+ \to K_S^0 K_S^0 e^+ \nu_e$, and $D^+ \to K^+ K^- e^+ \nu_e$ are selected from the remaining tracks in the presence of the tagged $\bar{D}$ candidates. We require that there are four, five, and three charged tracks ($N_{\mathrm{extra}}^{\mathrm{charge}}$) reconstructed in the $D^0 \to K_S^0 K^- e^+ \nu_e$, $D^+ \to K_S^0 K_S^0 e^+ \nu_e$, and $D^+ \to K^+ K^- e^+ \nu_e$ modes, respectively.

Candidates for $K^\pm$ and K_S^0 are selected with the same criteria as those used in the ST selection. A positron is identified using the measured information in the MDC, TOF, and EMC. The combined likelihoods ($\mathcal{L}'$) under the positron, pion, and kaon hypotheses are obtained. Positron candidates are required to satisfy $\mathcal{L}'(e) > 0.001$ and $\mathcal{L}'(e)/(\mathcal{L}'(e) + \mathcal{L}'(\pi) + \mathcal{L}'(K)) > 0.8$. To reduce background from hadrons and muons, the positron candidate is further required to have a deposited energy in the EMC greater than 0.8 times its momentum obtained in the MDC.

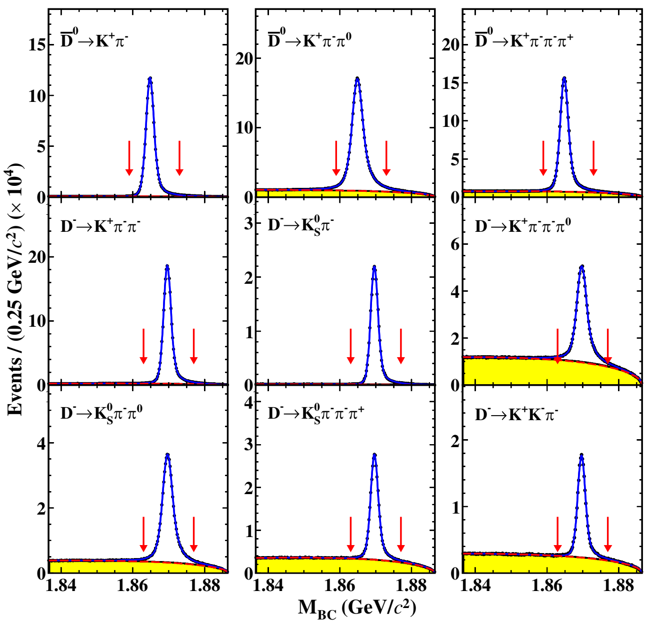

FIG. 2. Fits to the $M_{\rm BC}$ distributions of the ST $\bar{D}$ candidates. In each plot, the points with error bars correspond to the data, the blue curves are the best fits, and the red dashed curves describe the fitted combinatorial background shapes. The yellow normalization histograms show the scaled background contributions from the inclusive MC sample. The pair of red arrows indicate the $M_{\rm BC}$ signal window.

To suppress the backgrounds containing extra π^0 mesons, we require that there are no additional combinations of two photons ($N_{{\rm extra}\pi^0}$) that satisfy the requirements for a π^0 meson in the event selection. To reject contamination from the hadronic decays involving a π^0, e.g., $D^0 \to K_S^0 K^-\pi^+\pi^0$, $D^+ \to K_S^0 K_S^0 \pi^+\pi^0$, $D^+ \to K^+K^-\pi^+\pi^0$, the maximum energy of any extra photon ($E^{\rm max}_{{\rm extra}\gamma}$) which have not been used in the event selection are required to be less than 0.20, 0.17, and 0.25 GeV for $D^0 \to K_S^0 K^- e^+\nu_e$, $D^+ \to K_S^0 K_S^0 e^+\nu_e$, and $D^+ \to K^+K^- e^+\nu_e$, respectively. To suppress the backgrounds from the hadronic decays $D^0 \to K^-\pi^+\pi^+\pi^-$, $D^+ \to 2(\pi^+\pi^-)\pi^+$, and $D^+ \to K^+K^-\pi^+$, the invariant masses of the $K\bar{K}e$ combinations are required to be less than 1.74, 1.77, and 1.75 GeV/c^2 for $D^0 \to K_S^0 K^- e^+\nu_e$, $D^+ \to K_S^0 K_S^0 e^+\nu_e$, and $D^+ \to K^+K^- e^+\nu_e$, respectively. An additional requirement is deployed in the selection of $D^+ \to K^+K^- e^+\nu_e$ events, to suppress the background from $D^+ \to K^+K^-\pi^+\pi^0$ decays due to misidentifying a pion as an electron: the opening angle between the missing momentum and the most energetic shower, $\theta_{\vec{p}_{\rm miss},\gamma}$, is required to satisfy $\cos\theta_{\vec{p}_{\rm miss},\gamma} < 0.86$. These requirements have been optimized according to the Punzi criterion [29].

Events containing neutrinos cannot be fully reconstructed. To select semileptonic signal candidates, we define $U_{\rm miss} \equiv E_{\rm miss} - |\vec{p}_{\rm miss}|c$, where $E_{\rm miss}$ and $\vec{p}_{\rm miss}$ are the missing energy and momentum of the DT event in the e^+e^- center-of-mass frame, respectively. These quantities are calculated by $E_{\rm miss} \equiv E_{\rm beam} - E_{K_S^0(K_S^0)(K^+)} - E_{K^-(K_S^0)(K^-)} - E_{e^+}$ and $\vec{p}_{\rm miss} \equiv \vec{p}_D - \vec{p}_{K_S^0(K_S^0)(K^+)} - \vec{p}_{K^-(K_S^0)(K^-)} - \vec{p}_{e^+}$, where $E_{K_S^0(K^+)(K^-)(e^+)}$ and $\vec{p}_{K_S^0(K^+)(K^-)(e^+)}$ are the measured energy and momentum of the $K_S^0(K^+)(K^-)(e^+)$ candidates, respectively, and $\vec{p}_D \equiv -\hat{p}_{\bar{D}}\sqrt{E^2_{\rm beam}/c^2 - m^2_{\bar{D}}c^2}$, where $\hat{p}_{\bar{D}}$ is the unit vector in the momentum direction of the ST $\bar{D}$ meson and $m_{\bar{D}}$ is the known $\bar{D}$ mass [1]. For the decays $D^0 \to K_S^0 K^- e^+\nu_e$ and $D^+ \to K^+K^- e^+\nu_e$, the backgrounds from $D^0 \to K_S^0\pi^- e^+\nu_e$ or $D^+ \to \pi^+K^- e^+\nu_e$ due to the misidentification of the kaon are suppressed with the requirement of $0.16 < U^\pi_{\rm miss} < 0.31$ GeV and $0.17 < U^\pi_{\rm miss} < 0.32$ GeV, where $E^\pi_{\rm miss}$ and $U^\pi_{\rm miss}$ are calculated by replacing the K mass with the π mass in the previously defined quantities. Here, the beam energy and the nominal $\bar{D}$ mass are used to improve the $U_{\rm miss}$ resolution.

The average signal efficiencies in the presence of the ST $\bar{D}$ mesons are $(11.06 \pm 0.07)\%$, $(8.51 \pm 0.06)\%$, and $(13.06 \pm 0.07)\%$ for $D^0 \to K_S^0 K^- e^+\nu_e$, $D^+ \to K_S^0 K_S^0 e^+\nu_e$, and $D^+ \to K^+K^- e^+\nu_e$, respectively. These efficiencies do not include the BF of $K_S^0 \to \pi^+\pi^-$.

VI. RESULTS

Figure 3 shows the $U_{\rm miss}$ distributions of the candidate events for $D^0 \to K_S^0 K^- e^+\nu_e$, $D^+ \to K_S^0 K_S^0 e^+\nu_e$, and $D^+ \to K^+K^- e^+\nu_e$ selected from data. The signal yields are obtained by counting the events in the $U_{\rm miss}$ signal regions. Based on the MC study, the signal regions are defined as $[-0.041, 0.043]$, $[-0.042, 0.043]$, and $[-0.043, 0.046]$ GeV for $D^0 \to K_S^0 K^- e^+\nu_e$, $D^+ \to K_S^0 K_S^0 e^+\nu_e$, and $D^+ \to K^+K^- e^+\nu_e$, respectively, which correspond to intervals that are three times the resolution of the signal peaks. The yields in the signal regions ($N^{\rm sig}$) of the candidates for $D^0 \to K_S^0 K^- e^+\nu_e$, $D^+ \to K_S^0 K_S^0 e^+\nu_e$, and $D^+ \to K^+K^- e^+\nu_e$ are determined to be 9, 1, and 9, respectively. Based on the inclusive MC sample, the background yields ($N^{\rm bkg}$) are estimated to be 4.5 ± 2.1, 1.1 ± 1.0, and 3.5 ± 1.9 for $D^0 \to K_S^0 K^- e^+\nu_e$, $D^+ \to K_S^0 K_S^0 e^+\nu_e$, and $D^+ \to K^+K^- e^+\nu_e$, respectively.

Since no significant excesses are observed above background, we set the upper limits on the BFs of $D^0 \to K_S^0 K^- e^+\nu_e$, $D^+ \to K_S^0 K_S^0 e^+\nu_e$, and $D^+ \to K^+K^- e^+\nu_e$. Upper limits on the numbers of signal events at the 90% confidence level (CL) are calculated by using a frequentist method [30] with an unbound profile likelihood treatment of systematic uncertainties (see below), as implemented by the TRolke package in the ROOT software [31] with the quantities of $N^{\rm sig}$, $N^{\rm bkg}$, $\bar{\epsilon}_{\rm sig}$, and the total systematic uncertainty ($\delta_{\rm syst}$) as input. Here, the numbers of the signal and background events are assumed to follow a Poisson distribution, while the detection

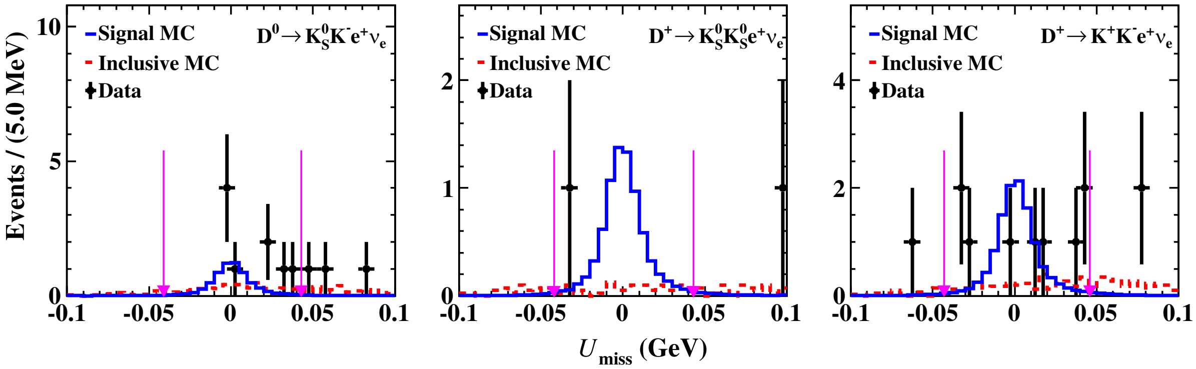

FIG. 3. The $U_{\rm miss}$ distributions of the accepted candidate events for $D^0 \to K_S^0 K^- e^+ \nu_e$, $D^+ \to K_S^0 K_S^0 e^+ \nu_e$, and $D^+ \to K^+ K^- e^+ \nu_e$. The dots with error bars are data, the blue histograms are the signal MC samples normalized with a product BF of 2×10^{-4} and the red dashed lines are the inclusive MC sample. The regions inside the pair of magenta arrows denote the signal regions.

efficiency is assumed to follow a Gaussian distribution. Finally, the upper limits on the BFs of $D^0 \to K_S^0 K^- e^+ \nu_e$, $D^+ \to K_S^0 K_S^0 e^+ \nu_e$, and $D^+ \to K^+ K^- e^+ \nu_e$ at the 90% CL are set to be 2.13×10^{-5}, 1.54×10^{-5}, and 2.10×10^{-5}, respectively.

VII. SYSTEMATIC UNCERTAINTY

With the DT method, many systematic uncertainties associated with the ST selection cancel and do not affect the BF measurement.

The uncertainty associated with the ST yield $N_{\rm ST}^{\rm tot}$, is assigned as 0.1% after varying the signal, background shapes and floating the parameters of one Gaussian in the fit. The tracking and PID efficiencies of $e^\pm$ are studied with a control sample of radiative Bhabha events, and those of the $K^\pm$ are studied by analyzing DT $D^0\bar{D}^0(D^+D^-)$ events, where the control samples comprise hadronic decays of $D^0 \to K^-\pi^+$, $D^0 \to K^-\pi^+\pi^0$, $D^0 \to K^-\pi^+\pi^+\pi^-$ versus $D^0 \to K^+\pi^-$, $D^0 \to K^+\pi^-\pi^0$, $D^0 \to K^+\pi^-\pi^-\pi^+$ as well as $D^+ \to K^-\pi^+\pi^+$ versus $D^+ \to K^+\pi^-\pi^-$. The systematic uncertainty due to tracking is assigned as 1.0% for both $K^\pm$ and $e^\pm$; the systematic uncertainty due to PID is assigned as 1.0% for $K^\pm$ and $e^\pm$. The uncertainty from the K_S^0 reconstruction is 1.5%, which is obtained by studying control samples of $J/\psi \to K^*(892)^\pm K^\mp$ and $J/\psi \to \phi K_S^0 K^\pm \pi^\mp$ [32] decays.

The uncertainty in the BF of $K_S^0 \to \pi^+\pi^-$ is 0.1% [1]. The uncertainties due to the limited size of MC samples are 0.6%, 0.7%, and 0.5% for $D^0 \to K_S^0 K^- e^+ \nu_e$, $D^+ \to K_S^0 K_S^0 e^+ \nu_e$, and $D^+ \to K^+ K^- e^+ \nu_e$, respectively.

The signal MC samples in this study are generated using the generator, in which the $M_{K\bar{K}}$ propagator is parameterized with a Flatté formula [25]. To assess the uncertainty arising from this generator, we use alternative signal MC samples by varying the coupling constants (g_1 and g_2) by $\pm 1\sigma$ around their central values as reported in [25]. These alternative samples allow us to estimate the impact of the variation in the coupling constants on the simulation results. The maximum changes in the DT efficiency between the DIY MC samples and the alternative signal MC samples are assigned to be 2.7%, 1.1%, and 0.9% for $D^0 \to K_S^0 K^- e^+ \nu_e$, $D^+ \to K_S^0 K_S^0 e^+ \nu_e$, and $D^+ \to K^+ K^- e^+ \nu_e$, respectively.

The combined systematic uncertainties from the $E_{{\rm extra}\gamma}^{\rm max}$, $N_{{\rm extra}\pi^0}$, and $N_{\rm extra}^{\rm charge}$ requirements are estimated to be 1.6%, 2.0%, and 0.9% for $D^0 \to K_S^0 K^- e^+ \nu_e$, $D^+ \to K_S^0 K_S^0 e^+ \nu_e$, and $D^+ \to K^+ K^- e^+ \nu_e$, respectively, which are assigned from studies of DT samples of $D^0 \to K^- e^+ \nu_e$ and $D^+ \to K_S^0 e^+ \nu_e$ reconstructed versus the same ST modes used in the baseline analysis.

The uncertainties from the $M_{K\bar{K}e}$, $U_{\rm miss}^{\pi\to K}$, and $\cos\theta_{\vec{p}_{\rm miss},\gamma}$ requirements are obtained by varying their values by ± 10 MeV$/c^2$, ± 1 MeV, ± 0.01, respectively, following the method defined in Refs. [33–35]. The maximum changes of the BF upper limits are taken as the associated systematic uncertainties.

Due to the limited sample size, only the resonant $K\bar{K}$ contributions in $D^0 \to K_S^0 K^- e^+ \nu_e$, $D^+ \to K_S^0 K_S^0 e^+ \nu_e$, and $D^+ \to K^+ K^- e^+ \nu_e$ are considered. The associated systematic uncertainty is assigned by using the alternative signal MC samples, mixed with 20% of nonresonant $D \to K_S^0 K(K_S^0 K_S^0)(KK) e^+ \nu_e$ and 80% of $D \to a_0(980)(\to K_S^0 K(K_S^0 K_S^0)(KK)) e^+ \nu_e$ decays. This is a conservative estimation as the largest known nonresonant contribution in the charm sector is only about 6.0% in the $D^+ \to K^-\pi^+ e^+ \nu_e$ decay [36]. The differences between the nominal and alternative signal efficiencies, 5.1%, 5.0%, and 4.6%, are taken as the systematic uncertainties for the BFs of the decays $D^0 \to K_S^0 K^- e^+ \nu_e$, $D^+ \to K_S^0 K_S^0 e^+ \nu_e$, and $D^+ \to K^+ K^- e^+ \nu_e$, respectively. The uncertainties due to the BFs of the D^0 and D^+ decays and the cross sections of $D^0\bar{D}^0$ and D^+D^- are negligible.

The total systematic uncertainty is obtained by adding the individual components in quadrature, assuming that all

TABLE III. Relative systematic uncertainties ($\delta_{\rm syst}$, in %) in the BF measurements.

Source	$D^0 \to K_S^0 K^- e^+ \nu_e$	$D^+ \to K_S^0 K_S^0 e^+ \nu_e$	$D^+ \to K^+ K^- e^+ \nu_e$
$N_{\rm ST}^{\rm tot}$	0.1	0.1	0.1
K/e tracking	2.0	1.0	3.0
K/e PID	2.0	1.0	3.0
K_S^0 reconstruction	1.5	3.0	$\cdots$
Quoted $\mathcal{B}$	0.1	0.2	$\cdots$
MC sample size	0.6	0.7	0.5
MC generator	2.7	1.1	0.9
$E_{\rm extra\gamma}^{\rm max}$, $N_{\rm extra\pi^0}$, and $N_{\rm extra}^{\rm charge}$ requirements	1.6	2.0	0.9
$M_{K\bar{K}e^+}$ requirement	0.4	1.2	2.4
$U_{\rm miss}^{\pi}$ requirement	1.0	$\cdots$	0.5
$\cos\theta_{\vec{p}_{\rm miss},\gamma}$ requirement	$\cdots$	$\cdots$	2.0
Nonresonant $K\bar{K}e\nu_e$ component	5.1	5.0	4.6
Total	6.9	6.6	7.1

sources are uncorrelated. Table III summarizes the sources of the systematic uncertainties in the BF measurements.

VIII. SUMMARY

By analyzing 7.9 fb^{-1} of e^+e^- annihilation data taken at $\sqrt{s} = 3.773$ GeV, we search for the semileptonic decays $D^0 \to K_S^0 K^- e^+ \nu_e$, $D^+ \to K_S^0 K_S^0 e^+ \nu_e$, and $D^+ \to K^+ K^- e^+ \nu_e$. No significant signals are observed. The upper limits on the BFs of $D^0 \to K_S^0 K^- e^+ \nu_e$, $D^+ \to K_S^0 K_S^0 e^+ \nu_e$, and $D^+ \to K^+ K^- e^+ \nu_e$ are set to be 2.13×10^{-5}, 1.54×10^{-5}, and 2.10×10^{-5} at the 90% CL, respectively. These upper limits are comparable to the expected product BFs of the individual decays. An increased dataset corresponding to an integrated luminosity of 20 fb^{-1} taken at $\sqrt{s} = 3.773$ GeV at BESIII will be available in the near future [13,37,38]. This larger sample will offer an opportunity to further improve the sensitivity of the search for these semileptonic decays.

ACKNOWLEDGMENTS

The BESIII collaboration thanks the staff of BEPCII and the IHEP computing center for their strong support. This work is supported in part by National Key R&D Program of China under Grants No. 2023YFA1606000, No. 2020YFA0406400, and No. 2020YFA0406300; National Natural Science Foundation of China (NSFC) under Grants No. 11635010, No. 11735014, No. 11835012, No. 11935015, No. 11935016, No. 11935018, No. 11961141012, No. 12025502, No. 12035009, No. 12035013, No. 12061131003, No. 12192260, No. 12192261, No. 12192262, No. 12192263, No. 12192264, No. 12192265, No. 12221005, No. 12225509, and No. 12235017; the Chinese Academy of Sciences (CAS) Large-Scale Scientific Facility Program; the CAS Center for Excellence in Particle Physics (CCEPP); Joint Large-Scale Scientific Facility Funds of the NSFC and CAS under Contract No. U1832207; CAS Key Research Program of Frontier Sciences under Grants No. QYZDJ-SSW-SLH003 and No. QYZDJ-SSW-SLH040; 100 Talents Program of CAS; The Institute of Nuclear and Particle Physics (INPAC) and Shanghai Key Laboratory for Particle Physics and Cosmology; European Union's Horizon 2020 research and innovation programme under Marie Sklodowska-Curie Grant Agreement No. 894790; German Research Foundation DFG under Grant No. 455635585, Collaborative Research Center CRC 1044, FOR5327, GRK 2149; Istituto Nazionale di Fisica Nucleare, Italy; Ministry of Development of Turkey under Grant No. DPT2006K-120470; National Research Foundation of Korea under Grant No. NRF-2022R1A2C1092335; National Science and Technology fund of Mongolia; National Science Research and Innovation Fund (NSRF) via the Program Management Unit for Human Resources & Institutional Development, Research and Innovation of Thailand under Contract No. B16F640076; Polish National Science Centre under Grant No. 2019/35/O/ST2/02907; The Swedish Research Council; U.S. Department of Energy under Grant No. DE-FG02-05ER41374.

[1] R. L. Workman *et al.* (Particle Data Group), Prog. Theor. Exp. Phys. **2022**, 083C01 (2022).
[2] J. J. Dudek *et al.* (Hadron Spectrum Collaboration), Phys. Rev. D **93**, 094506 (2016).
[3] G. Janssen, B. C. Pearce, K. Holinde, and J. Speth, Phys. Rev. D **52**, 2690 (1995).
[4] T. Branz, T. Gutsche, and V. E. Lyubovitskij, Eur. Phys. J. A **37**, 303 (2008).
[5] T. Branz, T. Gutsche, and V. E. Lyubovitskij, Phys. Rev. D **78**, 114004 (2008).
[6] R. L. Jaffe, Phys. Rev. D **15**, 281 (1977).
[7] M. Ablikim *et al.* (BESIII Collaboration), Phys. Rev. Lett. **121**, 081802 (2018).
[8] R. M. Wang, Y. Qiao, Y. J. Zhang, X. D. Cheng, and Y. G. Xu, Phys. Rev. D **107**, 056022 (2022).
[9] N. N. Achasov, A. V. Kiselev, and G. N. Shestakov, Phys. Rev. D **102**, 016022 (2020).
[10] M. Ablikim *et al.* (BESIII Collaboration), Chin. Phys. C **37**, 123001 (2013); Phys. Lett. B **753**, 629 (2016). These articles described the integrated luminosity measurement for data taken in 2010 and 2011. The integrated luminosity for data taken in 2022 is determined via a similar procedure.
[11] M. Ablikim *et al.* (BESIII Collaboration), Nucl. Instrum. Methods Phys. Res., Sect. A **614**, 345 (2010).
[12] C. H. Yu *et al.*, *Proceedings of IPAC2016, Busan, Korea* (2016), 10.18429/JACoW-IPAC2016-TUYA01.
[13] M. Ablikim *et al.* (BESIII Collaboration), Chin. Phys. C **44**, 040001 (2020).
[14] J. Lu, Y. Xiao, and X. Ji, Radiat. Detect. Technol. Methods **4**, 337 (2020).
[15] J. W. Zhang, L. H. Wu, S. S. Sun *et al.*, Radiat. Detect. Technol. Methods **6**, 289 (2022).
[16] K. X. Huang *et al.*, Nucl. Sci. Tech. **33**, 142 (2022).
[17] X. Li *et al.*, Radiat. Detect. Technol. Methods **1**, 13 (2017); Y. X. Guo *et al.*, Radiat. Detect. Technol. Methods **1**, 15 (2017); P. Cao *et al.*, Nucl. Instrum. Methods Phys. Res., Sect. A **953**, 163053 (2020).
[18] S. Agostinelli *et al.* (GEANT4 Collaboration), Nucl. Instrum. Methods Phys. Res., Sect. A **506**, 250 (2003).
[19] S. Jadach, B. F. L. Ward, and Z. Was, Comput. Phys. Commun. **130**, 260 (2000); Phys. Rev. D **63**, 113009 (2001).
[20] D. J. Lange, Nucl. Instrum. Methods Phys. Res., Sect. A **462**, 152 (2001); R. G. Ping, Chin. Phys. C **32**, 599 (2008).
[21] J. C. Chen, G. S. Huang, X. R. Qi, D. H. Zhang, and Y. S. Zhu, Phys. Rev. D **62**, 034003 (2000).
[22] E. Richter-Was, Phys. Lett. B **303**, 163 (1993).
[23] D. V. Bugg, V. V. Anisovich, A. Sarantsev, and B. S. Zou, Phys. Rev. D **50**, 4412 (1994).
[24] D. V. Bugg, Phys. Rev. D **78**, 074023 (2008).
[25] M. Ablikim *et al.* (BESIII Collaboration), Phys. Rev. D **95**, 032002 (2017).
[26] R. M. Baltrusaitis *et al.* (MARK-III Collaboration), Phys. Rev. Lett. **56**, 2140 (1986); J. Adler *et al.* (MARK-III Collaboration), Phys. Rev. Lett. **60**, 89 (1988).
[27] M. Ablikim *et al.* (BESIII Collaboration), Phys. Lett. B **734**, 227 (2014).
[28] H. Albrecht *et al.* (ARGUS Collaboration), Phys. Lett. B **241**, 278 (1990).
[29] G. Punzi, arXiv:2011.11770.
[30] W. A. Rolke, A. M. Lopez, and J. Conrad, Nucl. Instrum. Methods Phys. Res., Sect. A **551**, 493 (2005).
[31] R. Brun and F. Rademakers, Nucl. Instrum. Methods Phys. Res., Sect. A **389**, 81 (1997).
[32] M. Ablikim *et al.* (BESIII Collaboration), Phys. Rev. D **92**, 112008 (2015).
[33] M. Ablikim *et al.* (BESIII Collaboration), Phys. Rev. D **96**, 111101 (2017).
[34] M. Ablikim *et al.* (BESIII Collaboration), Phys. Rev. Lett. **121**, 171803 (2018).
[35] M. Ablikim *et al.* (BESIII Collaboration), Phys. Rev. Lett. **127**, 131801 (2021).
[36] M. Ablikim *et al.* (BESIII Collaboration), Phys. Rev. D **94**, 032001 (2016).
[37] B. C. Ke, J. Koponen, H. B. Li, and Y. Zheng, Annu. Rev. Nucl. Part. Sci. **73**, 285 (2023).
[38] H. B. Li and X. R. Lyu, Natl. Sci. Rev. **8**, nwab181 (2021).

M. Ablikim,[1] M. N. Achasov,[4,b] P. Adlarson,[75] O. Afedulidis,[3] X. C. Ai,[80] R. Aliberti,[35] A. Amoroso,[74a,74c] M. R. An,[39] Q. An,[71,58] Y. Bai,[57] O. Bakina,[36] I. Balossino,[29a] Y. Ban,[46,g] H.-R. Bao,[63] V. Batozskaya,[1,44] K. Begzsuren,[32] N. Berger,[35] M. Berlowski,[44] M. Bertani,[28a] D. Bettoni,[29a] F. Bianchi,[74a,74c] E. Bianco,[74a,74c] A. Bortone,[74a,74c] I. Boyko,[36] R. A. Briere,[5] A. Brueggemann,[68] H. Cai,[76] X. Cai,[1,58] A. Calcaterra,[28a] G. F. Cao,[1,63] N. Cao,[1,63] S. A. Cetin,[62a] J. F. Chang,[1,58] W. L. Chang,[1,63] G. R. Che,[43] G. Chelkov,[36,a] C. Chen,[43] Chao Chen,[55] G. Chen,[1] H. S. Chen,[1,63] M. L. Chen,[1,58,63] S. J. Chen,[42] S. L. Chen,[45] S. M. Chen,[61] T. Chen,[1,63] X. R. Chen,[31,63] X. T. Chen,[1,63] Y. B. Chen,[1,58] Y. Q. Chen,[34] Z. J. Chen,[25,h] S. K. Choi,[10a] X. Chu,[43] G. Cibinetto,[29a] S. C. Coen,[3] F. Cossio,[74c] J. J. Cui,[50] H. L. Dai,[1,58] J. P. Dai,[78] A. Dbeyssi,[18] R. E. de Boer,[3] D. Dedovich,[36] Z. Y. Deng,[1] A. Denig,[35] I. Denysenko,[36] M. Destefanis,[74a,74c] F. De Mori,[74a,74c] B. Ding,[66,1] X. X. Ding,[46,g] Y. Ding,[40] Y. Ding,[34] J. Dong,[1,58] L. Y. Dong,[1,63] M. Y. Dong,[1,58,63] X. Dong,[76] M. C. Du,[1] S. X. Du,[80] Z. H. Duan,[42] P. Egorov,[36,a] Y. H. Fan,[45] J. Fang,[1,58] S. S. Fang,[1,63] W. X. Fang,[1] Y. Fang,[1] Y. Q. Fang,[1,58] R. Farinelli,[29a] L. Fava,[74b,74c] F. Feldbauer,[3] G. Felici,[28a] C. Q. Feng,[71,58] J. H. Feng,[59] Y. T. Feng,[71,58] K. Fischer,[69] M. Fritsch,[3] C. D. Fu,[1] J. L. Fu,[63] Y. W. Fu,[1] H. Gao,[63] Y. N. Gao,[46,g] Yang Gao,[71,58] S. Garbolino,[74c] I. Garzia,[29a,29b] P. T. Ge,[76] Z. W. Ge,[42] C. Geng,[59] E. M. Gersabeck,[67] A. Gilman,[69] K. Goetzen,[13] L. Gong,[40] W. X. Gong,[1,58] W. Gradl,[35] S. Gramigna,[29a,29b] M. Greco,[74a,74c] M. H. Gu,[1,58] Y. T. Gu,[15] C. Y. Guan,[1,63] Z. L. Guan,[22] A. Q. Guo,[31,63] L. B. Guo,[41]

M. J. Guo,[50] R. P. Guo,[49] Y. P. Guo,[12,f] A. Guskov,[36,a] J. Gutierrez,[27] K. L. Han,[63] T. T. Han,[1] W. Y. Han,[39] X. Q. Hao,[19] F. A. Harris,[65] K. K. He,[55] K. L. He,[1,63] F. H. Heinsius,[3] C. H. Heinz,[35] Y. K. Heng,[1,58,63] C. Herold,[60] T. Holtmann,[3] P. C. Hong,[12,f] G. Y. Hou,[1,63] X. T. Hou,[1,63] Y. R. Hou,[63] Z. L. Hou,[1] B. Y. Hu,[59] H. M. Hu,[1,63] J. F. Hu,[56,i] T. Hu,[1,58,63] Y. Hu,[1] G. S. Huang,[71,58] K. X. Huang,[59] L. Q. Huang,[31,63] X. T. Huang,[50] Y. P. Huang,[1] T. Hussain,[73] F. Hölzken,[3] N. Hüsken,[27,35] N. in der Wiesche,[68] M. Irshad,[71,58] J. Jackson,[27] S. Jaeger,[3] S. Janchiv,[32] J. H. Jeong,[10a] Q. Ji,[1] Q. P. Ji,[19] X. B. Ji,[1,63] X. L. Ji,[1,58] Y. Y. Ji,[50] X. Q. Jia,[50] Z. K. Jia,[71,58] H. B. Jiang,[76] P. C. Jiang,[46,g] S. S. Jiang,[39] T. J. Jiang,[16] X. S. Jiang,[1,58,63] Y. Jiang,[63] J. B. Jiao,[50] Z. Jiao,[23] S. Jin,[42] Y. Jin,[66] M. Q. Jing,[1,63] X. M. Jing,[63] T. Johansson,[75] X. Kui,[1] S. Kabana,[33] N. Kalantar-Nayestanaki,[64] X. L. Kang,[9] X. S. Kang,[40] M. Kavatsyuk,[64] B. C. Ke,[80] V. Khachatryan,[27] A. Khoukaz,[68] R. Kiuchi,[1] O. B. Kolcu,[62a] B. Kopf,[3] M. Kuessner,[3] A. Kupsc,[44,75] W. Kühn,[37] J. J. Lane,[67] P. Larin,[18] L. Lavezzi,[74a,74c] T. T. Lei,[71,58] Z. H. Lei,[71,58] H. Leithoff,[35] M. Lellmann,[35] T. Lenz,[35] C. Li,[43] C. Li,[47] C. H. Li,[39] Cheng Li,[71,58] D. M. Li,[80] F. Li,[1,58] G. Li,[1] H. Li,[71,58] H. B. Li,[1,63] H. J. Li,[19] H. N. Li,[56,i] Hui Li,[43] J. R. Li,[61] J. S. Li,[59] J. W. Li,[50] Ke Li,[1] L. J. Li,[1,63] L. K. Li,[1] Lei Li,[48] M. H. Li,[43] P. R. Li,[38,k] Q. X. Li,[50] S. X. Li,[12] T. Li,[50] W. D. Li,[1,63] W. G. Li,[1] X. H. Li,[71,58] X. L. Li,[50] Xiaoyu Li,[1,63] Y. G. Li,[46,g] Z. J. Li,[59] Z. X. Li,[15] C. Liang,[42] H. Liang,[1,63] H. Liang,[71,58] Y. F. Liang,[54] Y. T. Liang,[31,63] G. R. Liao,[14] L. Z. Liao,[50] Y. P. Liao,[1,63] J. Libby,[26] A. Limphirat,[60] D. X. Lin,[31,63] T. Lin,[1] B. J. Liu,[1] B. X. Liu,[76] C. Liu,[34] C. X. Liu,[1] F. H. Liu,[53] Fang Liu,[1] Feng Liu,[6] G. M. Liu,[56,i] H. Liu,[38,j,k] H. B. Liu,[15] H. M. Liu,[1,63] Huanhuan Liu,[1] Huihui Liu,[21] J. B. Liu,[71,58] J. Y. Liu,[1,63] K. Liu,[38,j,k] K. Y. Liu,[40] Ke Liu,[22] L. Liu,[71,58] L. C. Liu,[43] Lu Liu,[43] M. H. Liu,[12,f] P. L. Liu,[1] Q. Liu,[63] S. B. Liu,[71,58] T. Liu,[12,f] W. K. Liu,[43] W. M. Liu,[71,58] X. Liu,[38,j,k] Y. Liu,[80] Y. Liu,[38,j,k] Y. B. Liu,[43] Z. A. Liu,[1,58,63] Z. Q. Liu,[50] X. C. Lou,[1,58,63] F. X. Lu,[59] H. J. Lu,[23] J. G. Lu,[1,58] X. L. Lu,[1] Y. Lu,[7] Y. P. Lu,[1,58] Z. H. Lu,[1,63] C. L. Luo,[41] M. X. Luo,[79] T. Luo,[12,f] X. L. Luo,[1,58] X. R. Lyu,[63] Y. F. Lyu,[43] F. C. Ma,[40] H. Ma,[78] H. L. Ma,[1] J. L. Ma,[1,63] L. L. Ma,[50] M. M. Ma,[1,63] Q. M. Ma,[1] R. Q. Ma,[1,63] X. Y. Ma,[1,58] Y. Ma,[46,g] Y. M. Ma,[31] F. E. Maas,[18] M. Maggiora,[74a,74c] S. Malde,[69] A. Mangoni,[28b] Y. J. Mao,[46,g] Z. P. Mao,[1] S. Marcello,[74a,74c] Z. X. Meng,[66] J. G. Messchendorp,[13,64] G. Mezzadri,[29a] H. Miao,[1,63] T. J. Min,[42] R. E. Mitchell,[27] X. H. Mo,[1,58,63] B. Moses,[27] N. Yu. Muchnoi,[4,b] J. Muskalla,[35] Y. Nefedov,[36] F. Nerling,[18,d] I. B. Nikolaev,[4,b] Z. Ning,[1,58] S. Nisar,[11,l] Q. L. Niu,[38,j,k] W. D. Niu,[55] Y. Niu,[50] S. L. Olsen,[63] Q. Ouyang,[1,58,63] S. Pacetti,[28b,28c] X. Pan,[55] Y. Pan,[57] A. Pathak,[34] P. Patteri,[28a] Y. P. Pei,[71,58] M. Pelizaeus,[3] H. P. Peng,[71,58] Y. Y. Peng,[38,j,k] K. Peters,[13,d] J. L. Ping,[41] R. G. Ping,[1,63] S. Plura,[35] V. Prasad,[33] F. Z. Qi,[1] H. Qi,[71,58] H. R. Qi,[61] M. Qi,[42] T. Y. Qi,[12,f] S. Qian,[1,58] W. B. Qian,[63] C. F. Qiao,[63] J. J. Qin,[72] L. Q. Qin,[14] X. S. Qin,[50] Z. H. Qin,[1,58] J. F. Qiu,[1] S. Q. Qu,[61] C. F. Redmer,[35] K. J. Ren,[39] A. Rivetti,[74c] M. Rolo,[74c] G. Rong,[1,63] Ch. Rosner,[18] S. N. Ruan,[43] N. Salone,[44] A. Sarantsev,[36,c] Y. Schelhaas,[35] K. Schoenning,[75] M. Scodeggio,[29a,29b] K. Y. Shan,[12,f] W. Shan,[24] X. Y. Shan,[71,58] J. F. Shangguan,[55] L. G. Shao,[1,63] M. Shao,[71,58] C. P. Shen,[12,f] H. F. Shen,[1,63] W. H. Shen,[63] X. Y. Shen,[1,63] B. A. Shi,[63] H. C. Shi,[71,58] J. L. Shi,[12] J. Y. Shi,[1] Q. Q. Shi,[55] R. S. Shi,[1,63] X. Shi,[1,58] J. J. Song,[19] T. Z. Song,[59] W. M. Song,[34,1] Y. J. Song,[12] S. Sosio,[74a,74c] S. Spataro,[74a,74c] F. Stieler,[35] Y. J. Su,[63] G. B. Sun,[76] G. X. Sun,[1] H. Sun,[63] H. K. Sun,[1] J. F. Sun,[19] K. Sun,[61] L. Sun,[76] S. S. Sun,[1,63] T. Sun,[51,e] W. Y. Sun,[34] Y. Sun,[9] Y. J. Sun,[71,58] Y. Z. Sun,[1] Z. T. Sun,[50] Y. X. Tan,[71,58] C. J. Tang,[54] G. Y. Tang,[1] J. Tang,[59] Y. A. Tang,[76] L. Y. Tao,[72] Q. T. Tao,[25,h] M. Tat,[69] J. X. Teng,[71,58] V. Thoren,[75] W. H. Tian,[52] W. H. Tian,[59] Y. Tian,[31,63] Z. F. Tian,[76] I. Uman,[62b] Y. Wan,[55] S. J. Wang,[50] B. Wang,[1] B. L. Wang,[63] Bo Wang,[71,58] C. W. Wang,[42] D. Y. Wang,[46,g] F. Wang,[72] H. J. Wang,[38,j,k] J. P. Wang,[50] K. Wang,[1,58] L. L. Wang,[1] M. Wang,[50] Meng Wang,[1,63] N. Y. Wang,[63] S. Wang,[12,f] S. Wang,[38,j,k] T. Wang,[12,f] T. J. Wang,[43] W. Wang,[59] W. Wang,[72] W. P. Wang,[71,58] X. Wang,[46,g] X. F. Wang,[38,j,k] X. J. Wang,[39] X. L. Wang,[12,f] Y. Wang,[61] Y. D. Wang,[45] Y. F. Wang,[1,58,63] Y. L. Wang,[19] Y. N. Wang,[45] Y. Q. Wang,[1] Yaqian Wang,[17] Yi Wang,[61] Z. Wang,[1,58] Z. L. Wang,[72] Z. Y. Wang,[1,63] Ziyi Wang,[63] D. Wei,[70] D. H. Wei,[14] F. Weidner,[68] S. P. Wen,[1] C. Wenzel,[3] U. Wiedner,[3] G. Wilkinson,[69] M. Wolke,[75] L. Wollenberg,[3] C. Wu,[39] J. F. Wu,[1,8] L. H. Wu,[1] L. J. Wu,[1,63] X. Wu,[12,f] X. H. Wu,[34] Y. Wu,[71] Y. H. Wu,[55] Y. J. Wu,[31] Z. Wu,[1,58] L. Xia,[71,58] X. M. Xian,[39] T. Xiang,[46,g] D. Xiao,[38,j,k] G. Y. Xiao,[42] S. Y. Xiao,[1] Y. L. Xiao,[12,f] Z. J. Xiao,[41] C. Xie,[42] X. H. Xie,[46,g] Y. Xie,[50] Y. G. Xie,[1,58] Y. H. Xie,[6] Z. P. Xie,[71,58] T. Y. Xing,[1,63] C. F. Xu,[1,63] C. J. Xu,[59] G. F. Xu,[1] H. Y. Xu,[66] Q. J. Xu,[16] Q. N. Xu,[30] W. Xu,[1] W. L. Xu,[66] X. P. Xu,[55] Y. C. Xu,[77] Z. P. Xu,[42] Z. S. Xu,[63] F. Yan,[12,f] L. Yan,[12,f] W. B. Yan,[71,58] W. C. Yan,[80] X. Q. Yan,[1] H. J. Yang,[51,e] H. L. Yang,[34] H. X. Yang,[1] Tao Yang,[1] Y. Yang,[12,f] Y. F. Yang,[43] Y. X. Yang,[1,63] Yifan Yang,[1,63] Z. W. Yang,[38,j,k] Z. P. Yao,[50] M. Ye,[1,58] M. H. Ye,[8] J. H. Yin,[1] Z. Y. You,[59] B. X. Yu,[1,58,63] C. X. Yu,[43] G. Yu,[1,63] J. S. Yu,[25,h] T. Yu,[72] X. D. Yu,[46,g] C. Z. Yuan,[1,63] L. Yuan,[2] S. C. Yuan,[1] Y. Yuan,[1,63] Z. Y. Yuan,[59] C. X. Yue,[39] A. A. Zafar,[73] F. R. Zeng,[50] S. H. Zeng,[72] X. Zeng,[12,f] Y. Zeng,[25,h] Y. J. Zeng,[1,63] X. Y. Zhai,[34] Y. C. Zhai,[50] Y. H. Zhan,[59] A. Q. Zhang,[1,63] B. L. Zhang,[1,63] B. X. Zhang,[1] D. H. Zhang,[43] G. Y. Zhang,[19] H. Zhang,[71] H. C. Zhang,[1,58,63] H. H. Zhang,[34] H. H. Zhang,[59] H. Q. Zhang,[1,58,63] H. Y. Zhang,[1,58] J. Zhang,[80] J. Zhang,[59] J. J. Zhang,[52] J. L. Zhang,[20] J. Q. Zhang,[41] J. W. Zhang,[1,58,63]

J. X. Zhang,[38,j,k] J. Y. Zhang,[1] J. Z. Zhang,[1,63] Jianyu Zhang,[63] L. M. Zhang,[61] L. Q. Zhang,[59] Lei Zhang,[42] P. Zhang,[1,63] Q. Y. Zhang,[39,80] Shuihan Zhang,[1,63] Shulei Zhang,[25,h] X. D. Zhang,[45] X. M. Zhang,[1] X. Y. Zhang,[50] Y. Zhang,[69] Y. Zhang,[72] Y. T. Zhang,[80] Y. H. Zhang,[1,58] Yan Zhang,[71,58] Yao Zhang,[1] Z. D. Zhang,[1] Z. H. Zhang,[1] Z. L. Zhang,[34] Z. Y. Zhang,[76] Z. Y. Zhang,[43] G. Zhao,[1] J. Y. Zhao,[1,63] J. Z. Zhao,[1,58] Lei Zhao,[71,58] Ling Zhao,[1] M. G. Zhao,[43] R. P. Zhao,[63] S. J. Zhao,[80] Y. B. Zhao,[1,58] Y. X. Zhao,[31,63] Z. G. Zhao,[71,58] A. Zhemchugov,[36,a] B. Zheng,[72] J. P. Zheng,[1,58] W. J. Zheng,[1,63] Y. H. Zheng,[63] B. Zhong,[41] X. Zhong,[59] H. Zhou,[50] L. P. Zhou,[1,63] X. Zhou,[76] X. K. Zhou,[6] X. R. Zhou,[71,58] X. Y. Zhou,[39] Y. Z. Zhou,[12,f] J. Zhu,[43] K. Zhu,[1] K. J. Zhu,[1,58,63] L. Zhu,[34] L. X. Zhu,[63] S. H. Zhu,[70] S. Q. Zhu,[42] T. J. Zhu,[12,f] W. J. Zhu,[12,f] Y. C. Zhu,[71,58] Z. A. Zhu,[1,63] J. H. Zou,[1] and J. Zu[71,58]

(BESIII Collaboration)

[1]*Institute of High Energy Physics, Beijing 100049, People's Republic of China*
[2]*Beihang University, Beijing 100191, People's Republic of China*
[3]*Bochum Ruhr-University, D-44780 Bochum, Germany*
[4]*Budker Institute of Nuclear Physics SB RAS (BINP), Novosibirsk 630090, Russia*
[5]*Carnegie Mellon University, Pittsburgh, Pennsylvania 15213, USA*
[6]*Central China Normal University, Wuhan 430079, People's Republic of China*
[7]*Central South University, Changsha 410083, People's Republic of China*
[8]*China Center of Advanced Science and Technology, Beijing 100190, People's Republic of China*
[9]*China University of Geosciences, Wuhan 430074, People's Republic of China*
[10]*Chung-Ang University, Seoul, 06974, Republic of Korea*
[11]*COMSATS University Islamabad, Lahore Campus, Defence Road, Off Raiwind Road, 54000 Lahore, Pakistan*
[12]*Fudan University, Shanghai 200433, People's Republic of China*
[13]*GSI Helmholtzcentre for Heavy Ion Research GmbH, D-64291 Darmstadt, Germany*
[14]*Guangxi Normal University, Guilin 541004, People's Republic of China*
[15]*Guangxi University, Nanning 530004, People's Republic of China*
[16]*Hangzhou Normal University, Hangzhou 310036, People's Republic of China*
[17]*Hebei University, Baoding 071002, People's Republic of China*
[18]*Helmholtz Institute Mainz, Staudinger Weg 18, D-55099 Mainz, Germany*
[19]*Henan Normal University, Xinxiang 453007, People's Republic of China*
[20]*Henan University, Kaifeng 475004, People's Republic of China*
[21]*Henan University of Science and Technology, Luoyang 471003, People's Republic of China*
[22]*Henan University of Technology, Zhengzhou 450001, People's Republic of China*
[23]*Huangshan College, Huangshan 245000, People's Republic of China*
[24]*Hunan Normal University, Changsha 410081, People's Republic of China*
[25]*Hunan University, Changsha 410082, People's Republic of China*
[26]*Indian Institute of Technology Madras, Chennai 600036, India*
[27]*Indiana University, Bloomington, Indiana 47405, USA*
[28a]*INFN Laboratori Nazionali di Frascati, INFN Laboratori Nazionali di Frascati, I-00044, Frascati, Italy*
[28b]*INFN Laboratori Nazionali di Frascati, INFN Sezione di Perugia, I-06100, Perugia, Italy*
[28c]*INFN Laboratori Nazionali di Frascati, University of Perugia, I-06100, Perugia, Italy*
[29a]*INFN Sezione di Ferrara, INFN Sezione di Ferrara, I-44122, Ferrara, Italy*
[29b]*INFN Sezione di Ferrara, University of Ferrara, I-44122, Ferrara, Italy*
[30]*Inner Mongolia University, Hohhot 010021, People's Republic of China*
[31]*Institute of Modern Physics, Lanzhou 730000, People's Republic of China*
[32]*Institute of Physics and Technology, Peace Avenue 54B, Ulaanbaatar 13330, Mongolia*
[33]*Instituto de Alta Investigación, Universidad de Tarapacá, Casilla 7D, Arica 1000000, Chile*
[34]*Jilin University, Changchun 130012, People's Republic of China*
[35]*Johannes Gutenberg University of Mainz, Johann-Joachim-Becher-Weg 45, D-55099 Mainz, Germany*
[36]*Joint Institute for Nuclear Research, 141980 Dubna, Moscow region, Russia*
[37]*Justus-Liebig-Universitaet Giessen, II. Physikalisches Institut, Heinrich-Buff-Ring 16, D-35392 Giessen, Germany*
[38]*Lanzhou University, Lanzhou 730000, People's Republic of China*
[39]*Liaoning Normal University, Dalian 116029, People's Republic of China*
[40]*Liaoning University, Shenyang 110036, People's Republic of China*
[41]*Nanjing Normal University, Nanjing 210023, People's Republic of China*
[42]*Nanjing University, Nanjing 210093, People's Republic of China*

[43]Nankai University, Tianjin 300071, People's Republic of China
[44]National Centre for Nuclear Research, Warsaw 02-093, Poland
[45]North China Electric Power University, Beijing 102206, People's Republic of China
[46]Peking University, Beijing 100871, People's Republic of China
[47]Qufu Normal University, Qufu 273165, People's Republic of China
[48]Renmin University of China, Beijing 100872, People's Republic of China
[49]Shandong Normal University, Jinan 250014, People's Republic of China
[50]Shandong University, Jinan 250100, People's Republic of China
[51]Shanghai Jiao Tong University, Shanghai 200240, People's Republic of China
[52]Shanxi Normal University, Linfen 041004, People's Republic of China
[53]Shanxi University, Taiyuan 030006, People's Republic of China
[54]Sichuan University, Chengdu 610064, People's Republic of China
[55]Soochow University, Suzhou 215006, People's Republic of China
[56]South China Normal University, Guangzhou 510006, People's Republic of China
[57]Southeast University, Nanjing 211100, People's Republic of China
[58]State Key Laboratory of Particle Detection and Electronics, Beijing 100049, Hefei 230026, People's Republic of China
[59]Sun Yat-Sen University, Guangzhou 510275, People's Republic of China
[60]Suranaree University of Technology, University Avenue 111, Nakhon Ratchasima 30000, Thailand
[61]Tsinghua University, Beijing 100084, People's Republic of China
[62a]Turkish Accelerator Center Particle Factory Group, Istinye University, 34010, Istanbul, Turkey
[62b]Turkish Accelerator Center Particle Factory Group, Near East University, Nicosia, North Cyprus, 99138, Mersin 10, Turkey
[63]University of Chinese Academy of Sciences, Beijing 100049, People's Republic of China
[64]University of Groningen, NL-9747 AA Groningen, The Netherlands
[65]University of Hawaii, Honolulu, Hawaii 96822, USA
[66]University of Jinan, Jinan 250022, People's Republic of China
[67]University of Manchester, Oxford Road, Manchester M13 9PL, United Kingdom
[68]University of Muenster, Wilhelm-Klemm-Strasse 9, 48149 Muenster, Germany
[69]University of Oxford, Keble Road, Oxford OX13RH, United Kingdom
[70]University of Science and Technology Liaoning, Anshan 114051, People's Republic of China
[71]University of Science and Technology of China, Hefei 230026, People's Republic of China
[72]University of South China, Hengyang 421001, People's Republic of China
[73]University of the Punjab, Lahore-54590, Pakistan
[74a]University of Turin and INFN, University of Turin, I-10125, Turin, Italy
[74b]University of Turin and INFN, University of Eastern Piedmont, I-15121, Alessandria, Italy
[74c]University of Turin and INFN, INFN, I-10125, Turin, Italy
[75]Uppsala University, Box 516, SE-75120 Uppsala, Sweden
[76]Wuhan University, Wuhan 430072, People's Republic of China
[77]Yantai University, Yantai 264005, People's Republic of China
[78]Yunnan University, Kunming 650500, People's Republic of China
[79]Zhejiang University, Hangzhou 310027, People's Republic of China
[80]Zhengzhou University, Zhengzhou 450001, People's Republic of China

[a]Also at the Moscow Institute of Physics and Technology, Moscow 141700, Russia.
[b]Also at the Novosibirsk State University, Novosibirsk, 630090, Russia.
[c]Also at the NRC "Kurchatov Institute," PNPI, 188300, Gatchina, Russia.
[d]Also at Goethe University Frankfurt, 60323 Frankfurt am Main, Germany.
[e]Also at Key Laboratory for Particle Physics, Astrophysics and Cosmology, Ministry of Education; Shanghai Key Laboratory for Particle Physics and Cosmology; Institute of Nuclear and Particle Physics, Shanghai 200240, People's Republic of China.
[f]Also at Key Laboratory of Nuclear Physics and Ion-beam Application (MOE) and Institute of Modern Physics, Fudan University, Shanghai 200443, People's Republic of China.
[g]Also at State Key Laboratory of Nuclear Physics and Technology, Peking University, Beijing 100871, People's Republic of China.
[h]Also at School of Physics and Electronics, Hunan University, Changsha 410082, China.
[i]Also at Guangdong Provincial Key Laboratory of Nuclear Science, Institute of Quantum Matter, South China Normal University, Guangzhou 510006, China.
[j]Also at MOE Frontiers Science Center for Rare Isotopes, Lanzhou University, Lanzhou 730000, People's Republic of China.
[k]Also at Lanzhou Center for Theoretical Physics, Lanzhou University, Lanzhou 730000, People's Republic of China.
[l]Also at the Department of Mathematical Sciences, IBA, Karachi 75270, Pakistan.